Observation of a Molecular Frame (*e, 2e*) Cross Section: An (*e, 2e* + *M*) Triple Coincidence Study on H₂

M. Takahashi,[1,2,*] N. Watanabe,[1,2] Y. Khajuria,[1] Y. Udagawa,[2] and J. H. D. Eland[3]

[1]*Institute for Molecular Science, Okazaki 444-8585, Japan*
[2]*Institute of Multidisciplinary Research for Advanced Materials, Tohoku University, Sendai 980-8577, Japan*
[3]*Physical and Theoretical Chemistry Laboratory, Oxford University, Oxford OX1 3QZ, United Kingdom*

We report the first experimental results showing transition-specific anisotropy of molecular frame (*e, 2e*) cross sections. Vector correlations between the two outgoing electrons and the fragment ion have been measured for specific ionization-excitation processes of H_2. The results enable us to obtain molecular frame (*e, 2e*) cross sections for transitions to the $2s\sigma_g$ and $2p\sigma_u$ excited states of H_2^+, thereby making stereodynamics of the electron-molecule collisions directly visible.

Binary (*e, 2e*) spectroscopy or electron momentum spectroscopy (EMS) is a powerful tool for investigating the electronic structure of matter [1–4]. Since the pioneering work by Amaldi *et al.* on a thin carbon film in 1969 [5] and later by Weigold *et al.* on Ar in 1973 [6], EMS has been applied to various targets involving laser excited oriented atoms, biomolecules, and solids [4]. In particular, its unique ability to look at individual electronic orbitals in momentum space, along with its many important applications in quantum chemistry, has been widely exploited in the last three decades [3,4], with the aid of plane-wave impulse approximation (PWIA) calculations [1,2].

For molecules, however, EMS has long been plagued by the fact that the experiments measure averages over all orientations of gaseous targets. The spherical averaging results in enormous loss of versatile information on collision dynamics and target electronic structure; intrinsically anisotropic or three-dimensional character of the (*e, 2e*) scattering by molecules deteriorates into the one-dimensional momentum distribution or momentum profile. If it were possible to fix a molecule in space, the experiment would remove ambiguities inherent in the analysis of the spherically averaged (*e, 2e*) cross sections and directly provide information important to momentum space chemistry [7,8] as well as to collision physics.

Very recently, we have developed a multichannel apparatus [9] to measure the (*e, 2e*) cross section in the molecular frame by the use of ion fragmentation with axial recoil [10]; if the molecular ion dissociates much faster than it rotates, the direction of fragment ion departure coincides with the molecular orientation at the moment of the ionization. EMS experiments in conjunction with axial recoil fragmentation, which can be designated as the (*e, 2e* + *M*) method, become possible only by measurement of vector correlations between the two outgoing electrons and the fragment ion by a triple coincidence technique.

In this Letter we report the first observation of transition-specific anisotropy in molecular frame (*e, 2e*) spectroscopy by means of the (*e, 2e* + *M*) method. In our preliminary

study [9], the (*e, 2e*) cross section of H_2 was measured in the molecular frame, but it included contributions from several ionization transitions and no specific feature of any individual transitions was observed. In the present work, molecular frame (*e, 2e*) cross sections characteristic of the individual transitions to the $2s\sigma_g$ and $2p\sigma_u$ excited states of H_2^+ are reported. The results demonstrate a geometry effect of molecular orientation on the (*e, 2e*) amplitude and how it depends on the nature of the final ion state.

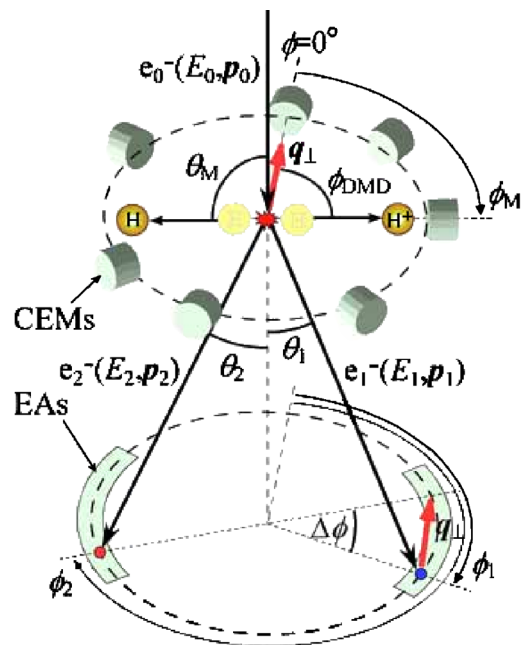The (*e, 2e* + *M*) experiment on H_2 was carried out at an impact energy of 1200 eV using the multichannel appara-

FIG. 1 (color online). Schematic of an (*e, 2e* + *M*) experimental setup based on the binary (*e, 2e*) scattering in the symmetric noncoplanar geometry, showing seven channel-electron multipliers (CEMs), and a pair of entrance apertures (EAs) of a spherical analyzer followed by a pair of position-sensitive detectors.

tus, of which a detailed description is given elsewhere [9] together with an account of the data reduction; only a brief account is given here. Figure 1 shows a schematic diagram of the experimental setup. Here the symmetric noncoplanar geometry is employed, in which two outgoing electrons having equal energies ($E_1 = E_2$) and equal polar angles ($\theta_1 = \theta_2 = 45°$) with respect to the incident electron momentum vector p_0 are detected in coincidence. Electron impact ionization occurs where an incident electron beam collides with a gaseous H_2 target. Two outgoing electrons emerging at $\theta_1 = \theta_2 = 45°$ are selected by a pair of entrance apertures extending over the azimuthal angle ϕ_1 and ϕ_2 ranges from 70° to 110° and from 250° to 290°. Then the electrons are energy analyzed and detected by means of a spherical analyzer followed by a pair of position-sensitive detectors (not depicted in the figure). Fragment ions are detected by the time-of-flight (TOF) technique using seven channel-electron multipliers (CEMs) placed in the plane ($\theta_M = 90°$) perpendicular to p_0. The azimuthal angular positions (ϕ_M's) of the CEMs are 0°, 45°, 90°, 150°, 195°, 240°, and 285°. A retarding electric field is applied in front of each CEM to collect only axial recoil fragments with large kinetic energies.

In the symmetric noncoplanar geometry, the magnitude of the recoil momentum q of the residual H_2^+ ion, before dissociation, is described by the following equation [2–4]:

$$q = \sqrt{(p_0 - \sqrt{2}p_1)^2 + [\sqrt{2}p_1 \sin(\Delta\phi/2)]^2}. \quad (1)$$

Here p_0 and p_1 are magnitudes of the momenta of the incident electron and one of the two outgoing electrons, and $\Delta\phi$ ($= \phi_2 - \phi_1 - \pi$) is the azimuthal angle difference between the two outgoing electrons. Equation (1) tells us that at sufficiently high impact energy where $p_0 \approx \sqrt{2}p_1$ the recoil momentum vector q is dominated by its component [$q_\perp, q_\perp = \sqrt{2}p_1 \sin(\Delta\phi/2)$] perpendicular to p_0, i.e., $q \approx q_\perp$. Moreover, in our experimental setup that covers the ϕ_1 and ϕ_2 ranges, the percentage of q's pointing within ±10° from the $\phi = 0°$ or 180° directions is about 74%, and that within ±15° is more than 90%. Hence, keeping in mind that the homonuclear target H_2 has inversion symmetry [molecular frame ($e, 2e$) cross section $\sigma(q)$ is equal to $\sigma(-q)$], ϕ_M can be approximated as the angle ϕ_{DMD} of q from the molecular axis, i.e., $\phi_M \approx \phi_{DMD}$. Thus the experimental setup makes it possible to probe anisotropy or ϕ_{DMD} dependence of molecular frame ($e, 2e$) cross section in the case of $\theta_M = 90°$.

Since all the transitions to excited states of H_2^+ are followed by direct dissociation, there is no doubt that their fragmentation is largely axial, as demonstrated by photo-electron angular distribution measurements for fixed-in-space H_2 molecules [11,12]. Theoretical kinetic energy distributions (KEDs) of such axial recoil fragments from several of the excited ion states are shown in Fig. 2(a), which were obtained by applying the reflection approximation to Franck-Condon transition profiles calculated using the BCONT program [13] with the relevant potential

energy curves [14]. It can be seen that fragment H^+ ions with kinetic energies larger than about 3 eV are produced from the excited states of H_2^+. On the other hand, the $1s\sigma_g$ ground state of H_2^+ is known to produce fragments having relatively small kinetic energy up to 1 eV [12]. Thus a retarding voltage of 2.5 V was used for the ($e, 2e + M$) experiment to detect the axial recoil H^+ ions from the excited ion states only.

In Fig. 2(b) we show an experimental KED of H^+, calculated from observed times of flight of fragment ions detected in coincidence with the two outgoing electrons. In the calculations small momentum components perpendicular to the TOF axis, which originate in the finite acceptance angle of the ion detectors, are neglected. Nevertheless, the experimental result is qualitatively reproduced by a fit (solid line) using the theoretical KEDs (broken lines) for the $2s\sigma_g$, $2p\sigma_u$, and $2p\pi_u$ transitions, the first two of which have been found to be dominant over other binary ($e, 2e$) ionization-excitation processes [15–18]. Thus the experimental KED was used to check the quality of the measured ($e, 2e + M$) data, as discussed below.

First, the observed kinetic energy range was divided into three regions, as indicated by I, II, and III in Fig. 2(b). ($e, 2e + M$) binding energy spectra were subsequently generated by summing triple coincidence signals over the $\Delta\phi$ and ϕ_M ranges selectively accepting events associated with the H^+ kinetic energy corresponding to the regions I–III, as shown in Figs. 3(a)–3(c), respectively. Likewise, a summed ($e, 2e + M$) binding energy spectrum was generated using the contributions from the entire kinetic energy range covered, and is presented in Fig. 3(d) with bars to show the vertical ionization energies of the relevant transitions. The calculated Franck-Condon transition profiles were folded with the instrumental energy resolution of
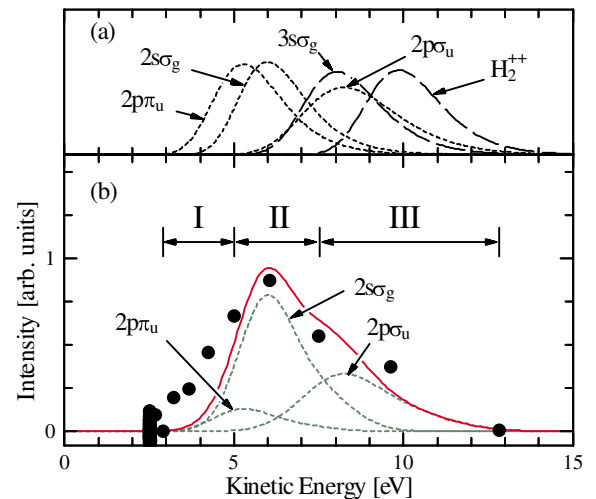

FIG. 2 (color online).   Calculated kinetic energy distributions of H^+ (a) and observed one (b). In the lower panel, results of a least-squares fit using the theoretical predictions for the $2s\sigma_g$, $2p\sigma_u$, and $2p\pi_u$ transitions are shown by broken lines. The solid line represents their sum.

about 7.6 eV (FWHM), and the resulting profiles were subsequently employed for deconvolution. The best fit to the experiment is shown in Fig. 3(d).

Figure 3 shows the results of energy correlation between the two outgoing electrons and the fragment ion. First, although the $(e, 2e)$ cross section for the transition to the $1s\sigma_g$ ground state of H_2^+ is several tens times larger than those for ionization-excitation processes [15–18], no peak corresponding to the $1s\sigma_g$ transition is observed in any spectrum of Fig. 3 because of the effect of the retarding field applied. Traces of the large cross section for the $1s\sigma_g$ transition are left in the relatively large error bars at around 16 eV. Second, since selection of the H^+ kinetic energy is equivalent to highlighting parts of the Franck-Condon transition profiles of particular transitions, specific ionization-excitation transitions predominate in Figs. 3(a)–3(c). The spectrum for selection I exhibits a peak at $\sim$36 eV and that for II at $\sim$39 eV; these peaks can be ascribed to the $2p\pi_u$ and $2s\sigma_g$ transitions, respectively. Similarly, the spectrum for region III shows a relatively large contribution of the $2p\sigma_u$ transition at $\sim$34 eV, together with some contributions from the transitions to $2s\sigma_g$ and higher excited ion states such as $3s\sigma_g$ and H_2^{++}. These observations confirm that successful measurements of vector correlations among the three charged particles have been achieved and that contributions of the individual ionization-excitation transitions can be extracted by deconvolution as in Fig. 3(d). A similar fitting procedure was repeated for a series of summed binding energy spectra at each angle ϕ_M to produce molecular frame $(e, 2e)$ cross sections, summed over the q range covered, for the dominant $2s\sigma_g$ and $2p\sigma_u$ transitions.

The molecular frame $(e, 2e)$ cross sections thus obtained for the two transitions are shown in Fig. 4, where they are plotted as a function of ϕ_{DMD} with the molecular axis drawn in the vertical direction. Here, by taking advantage of the inversion and rotation symmetry of the molecular frame $(e, 2e)$ cross sections about the molecular axis for a homonuclear molecule, the results are presented so as to give the 24 data points, whereas the measurement was performed at only seven ϕ_M's. Distance from the origin to each data point represents the relative magnitude of the cross section obtained at the corresponding angle ϕ_M.

Also included in the figure are associated PWIA predictions, shown by solid lines, which were obtained by calculating molecular frame electron momentum densities for the $2s\sigma_g$ and $2p\sigma_u$ transitions using a configuration-interaction H_2 wave function and by summing the momentum densities over the q range covered at each ϕ_{DMD}. To place the experiment and theory on a common intensity scale, we have used a normalization procedure similar to that in Ref. [9], as follows. Conventional spherically averaged $(e, 2e)$ data also are obtainable from the present $(e, 2e + M)$ measurement by the analysis of events where the two outgoing electrons are detected in coincidence but the fragment ion is in accidental coincidence. The idea
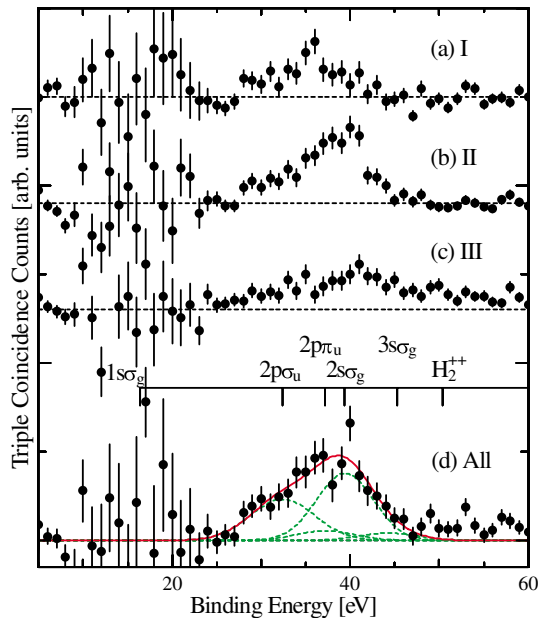

FIG. 3 (color online). $(e, 2e + M)$ binding energy spectra of H_2 associated with the H^+ kinetic energies corresponding to the regions (a) I, (b) II, (c) III, and (d) the entire range defined in Fig. 2(b). The broken and solid lines in (d) represent the deconvoluted curves and their sum.
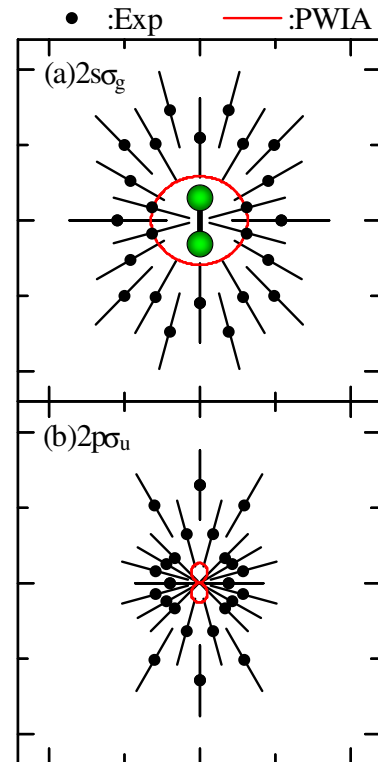

FIG. 4 (color online). Experimental molecular frame $(e, 2e)$ cross sections of H_2 for the transitions to the (a) $2s\sigma_g$ and (b) $2p\sigma_u$ excited ion states, obtained at an impact energy of 1200 eV. The molecular axis is in the vertical direction. The solid lines represent associated PWIA calculations.

used in the normalization procedure is that the strengths of the $2s\sigma_g$ and $2p\sigma_u$ transitions relative to the $1s\sigma_g$ transition are maintained in the $(e, 2e)$ data, and hence all the experimental momentum profiles (XMPs) can be placed on an absolute scale by fitting the area of the $1s\sigma_g$ XMP integrated over the entire q range to the PWIA $1s\sigma_g$ theoretical momentum profile (TMP). Note that the PWIA has been found to give a very good description of the $1s\sigma_g$ transition [15–18]. The ratio of the area of the absolute-scale $2s\sigma_g$ XMP to that of the $2s\sigma_g$ TMP has been estimated as 1.8, which is slightly larger than in the previous $(e, 2e)$ experiments [17,18]. Assuming the validity of this ratio for the $2s\sigma_g$ transition of the fixed-in-space H_2 molecules, the experimental $(e, 2e + M)$ $2s\sigma_g$ results are normalized in Fig. 4 so that their sum has the same ratio relative to the associated theoretical intensity. The normalization factor is applied to the experimental $(e, 2e + M)$ $2p\sigma_u$ results also. Thus all the molecular frame $(e, 2e)$ cross sections in Fig. 4 share a common intensity scale under the above assumption.

Although the statistics of the data leave much to be desired, one can see anisotropy of the molecular frame $(e, 2e)$ cross section that is peculiar to each ionization transition. Geometry effects of molecular orientation on the $(e, 2e)$ amplitudes are evident and the $2s\sigma_g$ and $2p\sigma_u$ experiments are strikingly different from each other. The former angular distribution is relatively isotropic, while the latter shows maxima along the molecular axis. This can be understood by considering the role of the first-order PWIA mechanism. It allows us to probe electron momentum densities of the $2s\sigma_g$ and $2p\sigma_u$ excited components involved because of electron correlation in the target H_2 wave function. Indeed, the PWIA calculations predict such angular distributions which reproduce qualitatively the shapes experimentally observed.

However, noticeable differences between experiments and PWIA calculations can be seen in intensity. For the $2p\sigma_u$ transition, in particular, the experimental results show several times larger intensity than the associated PWIA prediction. This is consistent with our previous $(e, 2e)$ study of H_2 [18], in which contributions of the second-order two-step (TS) mechanism [19,20] have been found to play a crucial role, especially in the $2p\sigma_u$ transition. Since the extent of the intensity difference between experiment and PWIA is a rough measure of contributions of the TS mechanism, the $2p\sigma_u$ results may offer one an opportunity to study geometry effects of molecular orientation in the mechanism. Unfortunately, poor statistics of the present data make it difficult to discuss such geometry effects, and hence we leave the issue for later experiments with improved data. Another promising direction would be to perform similar $(e, 2e + M)$ experiments for various linear molecules at high impact energy where the PWIA is valid, in order to look at three-dimensional molecular orbitals in momentum space.

In summary, we have reported the first observation of transition-specific anisotropy in molecular frame $(e, 2e)$ spectroscopy. The experimental results for the $2s\sigma_g$ and $2p\sigma_u$ transitions of H_2 are a visible proof of geometry effects of molecular orientation on the scattering amplitude depending upon the nature of each $(e, 2e)$ process. We believe that further attempts along this line would develop unexploited possibilities of the $(e, 2e)$ method, opening the door for detailed studies of bound electronic wave functions of molecules as well as of electron-molecule collision stereodynamics.

*Electronic addresses: masahiko@tagen.tohoku.ac.jp
masahiko@ims.ac.jp

[1] Yu. F. Smirnov and V. G. Neudatchin, JETP Lett. **3**, 192 (1966).

[2] I. E. McCarthy and E. Weigold, Phys. Rep. **C27**, 275 (1976).

[3] K. T. Leung, in *Theoretical Models of Chemical Bonding*, edited by Z. B. Maksic (Springer-Verlag, Berlin, 1991), Part 3.

[4] E. Weigold and I. E. McCarthy, *Electron Momentum Spectroscopy* (Kluwer Academic/Plenum Press, New York, 1999), and references therein.

[5] U. Amaldi, A. Egiri, R. Marconero, and P. Pizzella, Rev. Sci. Instrum. **40**, 1001 (1969).

[6] E. Weigold, S. T. Hood, and P. J. O. Teubner, Phys. Rev. Lett. **30**, 475 (1973).

[7] C. A. Coulson and W. E. Duncanson, Proc. Cambridge Philos. Soc. **37**, 55 (1941).

[8] I. R. Epstein and A. C. Tanner, in *Compton Scattering*, edited by B. G. Williams (McGraw-Hill, New York, 1977).

[9] M. Takahashi, N. Watanabe, Y. Khajuria, K. Nakayama, Y. Udagawa, and J. H. D. Eland, J. Electron Spectrosc. Relat. Phenom. **141**, 83 (2004).

[10] R. N. Zare, Mol. Photochem. **4**, 1 (1972).

[11] K. Ito, J. Adachi, R. Hall, S. Motoki, E. Shigemasa, K. Soejima, and A. Yagishita, J. Phys. B **33**, 527 (2000).

[12] Y. Hikosaka and J. H. D. Eland, Chem. Phys. **277**, 53 (2002).

[13] R. J. Le Roy, Comput. Phys. Commun. **52**, 383 (1989).

[14] T. E. Sharp, Atomic Data **2**, 119 (1971).

[15] E. Weigold, I. E. McCarthy, A. J. Dixson, and S. Dey, Chem. Phys. Lett. **47**, 209 (1977).

[16] S. M. Bharathi, S. Braidwood, A. M. Grisogono, N. Persiantseva, and E. Weigold, in *ICPEAC XVII Abstract* (Brisbane, Australia, 1991).

[17] N. Lermer, B. R. Todd, N. M. Cann, Y. Zheng, C. E. Brion, Z. Yang, and E. R. Davidson, Phys. Rev. A **56**, 1393 (1997).

[18] M. Takahashi, Y. Khajuria, and Y. Udagawa, Phys. Rev. A **68**, 042710 (2003).

[19] T. A. Carlson and M. O. Krause, Phys. Rev. **140**, A1057 (1965).

[20] R. J. Tweed, Z. Phys. D **23**, 309 (1992).